New Horizons in Earth Reinforcement – Otani, Miyata & Mukunoki (eds)
© 2008 Taylor & Francis Group, London, ISBN 978-0-415-45775-0

Stability analysis of a new type of reinforced earth slope

Y. Yokota
Maeda Kosen Co., Ltd., Fukui, Japan

K. Arai
University of Fukui, Fukui, Japan

S. Tsuji
Maeda Kosen Co., Ltd., Fukui, Japan

H. Ohta
Tokyo Institute of Technology, Tokyo, Japan

ABSTRACT: In 1999, a high and steep earth slope was constructed which have a maximum height of about 28 m and a slope gradient of 1:1.0. During the project, field observation was performed since the project involved widening of an old embankment that consisted of unknown soil (muck) in a steep topography with an elevation difference exceeding 50 m. To ensure the long-term stability of the embankment and protect the environment, TOGA wall method was applied, which reinforces the slopes by the compression force of geogrid reinforcements. TOGA is the name of place where the method was applied for the first time. The slope inclination and the arrangements of the reinforcements were determined using a standard manual of geogrid reinforced soil structures (Public Works Research Center, 2000). A FE analysis was carried out for predicting failure types by considering the deformation of the ground, and the analysis well duplicated the behaviors of the embankment monitored during the field observation. The results of FE analysis and the limit equilibrium method using circular slip surface method are compared to examine the validity of the soil parameter used for the embankment, and a design method to be used in the future is proposed.

1 INTRODUCTION

In 1999, a geogrid reinforced earth slope in which was 28 m high and 1:1.0 gradient of slope was designed and constructed as the widening of old embankment consisted of unknown soil (muck) in a steep topography. The usual slope gradient (1:1.5 to 1:2.0) would result in a bank extending long and spreading very wide at the toe of the slope, and would require a huge quantity of soil to bring in and adversely affect the natural environment. The bank was decided to be as tall as about 30 m, have a steep slope, and be constructed without excavating the natural ground. Since the geological and topographical conditions were complex and the bank was large, various methods were investigated to ensure the long-term stability. TOGA wall method was decided, which reinforces the bank slopes by the compression force of geogrid reinforcements. At the time, geogrid reinforcements had little been used as permanent structures of tall banks. Loosening of the soil, deformation of the slope, and surface failure during an earthquake and/or by seepage of rainwater were concerned for since the bank slopes could not be thoroughly compressed and the pressure of the bank was small. Thus, vertical compression force was applied to the slope sections of the terraced bank slope (each step had a height of 1 m, a width of 0.8 m, and a gradient of 1:0.2), to increase the soil density, control the expansion of soil volume during shear, and improve the shear resistance and stiffness.

The arrangements of geogrid (installation intervals and length) were determined using the standard manual of geogrid reinforced soil structures (called the standard manual), in which circular slip surface method is used. Cohesion was considered as a design parameter of the banking materials to reflect the reinforcement effects of TOGA wall method and the effects of rolling compaction. Compared with the result of a design made on a simple calculation of soil tests, TOGA wall design was very economic but was on the dangerous side. Thus, a field observation was conducted to examine the long-term stability of the bank.

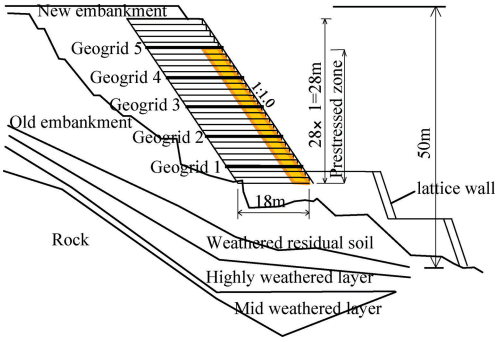

Figure 1. Cross section of TOGA wall.

This paper describes the results of a FE analysis carried out to estimate the failure types by considering the deformation of the ground and a comparison of the results with the data monitored in the field. The long-term stability of the bank was assessed also using data monitored in this study. The failure types determined by the FE analysis were compared with the results of the design method described in geogrid design manual using circular slip surface method. A design method to be used in the future is also proposed.

2 OUTLINE OF CONSTRUCTION

2.1 *Geogrid reinforced earth slope*

This project was executed as a part of a project for constructing a 317 m long highway. The project involved construction of TOGA wall of a height of 25 to 30 m, a lattice wall of a height of 15 m to 20 m, and cutting soil of about 50,000 m^3. A cross section of TOGA wall is shown Figure 1. The foundation ground was broadly classified into talus deposit, the old embankment and the natural ground. The old embankment was difficult to excavate since there were surplus earth and earth filling (SPT-N value is about 5 to 10) of the previous project extending over the embankment. The overall sliding through the old embankment or talus deposit was decided to be controlled by counterweight fill using lattice walls. The inclination of the bank slope of TOGA wall method was 1:1.0 to effectively use the earth discharged during the work and to ensure the stability as a permanent structure of high seismic performance and durability. The shape of the slope was decided to be terraced and consist of steps of a height of 1 m, a width of 0.8 m, and an inclination of 1:0.2 to structurally control compression force and protect the environment by planting vegetation as shown in Figure 2 (Ohta, H. et al., 2006).

TOGA wall has two features. One is the step form in which slope face consists of steel panel of 1 m high and flat area of 0.8 m wide. Another feature is, by adding compressive pre-stress vertically to the about 2 m area

Figure 2. Overall view of TOGA wall.

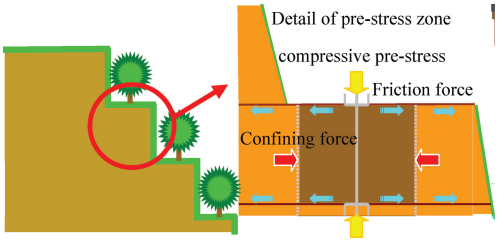

Figure 3. Mechanism of reinforcement.

sandwiched by geogrids in the flat area using steel plate and steel bar, to suppress volume expansion (positive dilatancy) generated at the occurrence of shearing deformation of the soil (Figure 3). The slope face helps maintenance as the space that is tense again when the pre-stress being relaxed. The embankment of the area sandwiched by geogrids and received pre-stress remarkably increase the shear resistance, and its ductility is drastically improved. A zone of this slope face acts as pseudo-wall of soil and adds shear resistance against slipping and retaining effect by the weight of wall surface body. As a result, from the generation of the apparent cohesive strength with the increase of slip protection force and the increase of lateral pressure, the decrease of necessary tensile strength of geogrid and the shortening of laying longitude are expected.

2.2 *Soil parameters of embankment and foundation ground*

Soil parameters used in the stability analysis are shown in Table 1. Where γ: unit weight, c: cohesion and ϕ: angle of shear resistance. For the embankment materials, direct shear test (constant volume) was carried out for the actual gravel soil used for banking. Considering long-term stability, the shear strength in drainage condition was used in the stability analysis. We determined the strength parameters of banking material considering effect of pseudo-wall of TOGA wall. Although cohesion of banking material $c = 0$ kN/m^2 determined by the direct

Table 1. Soil parameters.

	γ (kN/m^3)	c (kN/m^2)	ϕ (degree)
New embankment	19.0	0(30)	30.0
Old embankment	19.0	0	38.0
Weathered residual rock	18.5	50	23.3
Highly weathered layer	20.0	60	23.3
Mid weathered layer	20.0	70	23.3
Rock	23.0	0	42.5

Table 2. Comparison of design parameters.

Case 1 $\gamma = 19.0$ KN/m^3 c $= 30$ KN/m^2 $\phi = 30°$	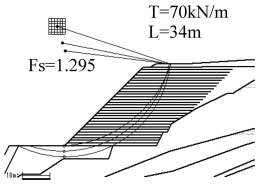
Case 2 $\gamma = 19.0$ KN/m^3 c $= 30$ KN/m^2 $\phi = 30°$	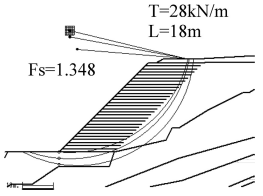

shear test, we assume to $c = 30$ kN/m^2 by considering confining effect and soil compaction effect of geogrid reinforced zone. We designed TOGA wall using strength parameters $c = 30$ kN/m^2 and $\phi = 30°$. The designs using $c = 0$ kN/m^2 and $c = 30$ kN/m^2 are compared in section 2.3. Validity of value of c is verified in section 4.3 by applying FE analysis and field observation. For the foundation ground, soil parameters were determined by laboratory test using undisturbed specimen and on standard penetration test.

2.3 *Geogrid arrangement*

As geogrid reinforcement, we used the aramid fiber reinforced geogrid. It has high strength, low ductility (4 to 6%), small deformation, and the design tensile strength of 27 kN/m. To determine the arrangement of the geogrids, a slope stability analysis was carried out which involved examining the inner stability against fracture and pull-out using the method described in the standard manual, and the overall stability was examined by investigating all slip surfaces including the slips in and outside the reinforced zone. Since the bank to built was as tall as $H = 28$ m, value of cohesion was changed from $c = 0$ kN/m^2 to $c = 30$ kN/m^2 in designing the earth slope since the former gave a very long geogrid length of $L = 34$ m, which was difficult to excavate. The results of the slope stability analysis are shown in Table 2 for each soil parameter.

Table 3. Results of field observation (Ohta, H. et al., 2006).

Tensile force of geogrid	Strain gauge	Force increases 9 kN/m during construction and reaches 32 kN/m after introducing prestress.
Force of steel Bar	Strain gauge	Force acting on steel bar is reduced to 1/3 after introducing prestress.
Earth pressure	Earth pressure meter	Horizontal earth pressure in the prestressed zone is smaller than active earth pressure calculated by earth pressure theory.
Displacement of foundation ground	Clinometer	Foundation ground deforms 50 mm horizontally.
Displacement of foundation ground	Optical distance measuring	Vertical displacement is 63 cm and horizontal displacement is 37 cm in middle part of slope.

2.4 *Field observation*

Field observation was carried out for 5 data items such as tensile force of geogrid, stress of steel bar for introduction of compressive force, vertical and horizontal earth pressures for each pre-stressed zone, displacement of the foundation ground and the toe of slope, and displacement of the slope face. The results of field observation at the completion of embankment are shown in Table 3.

3 NUMERICAL ANALYSIS

The soil is expressed as a plane strain element, and the shift between the soil and the wall blocks is expressed in an interface element. Mohr-Coulomb failure criterion is applied to the soil, and Coulomb failure criterion is applied to the interface element (Desai, C. S. et al. 1984).
Mohr-Coulomb:

$$F_M = \left\{\left(\sigma_x - \sigma_y\right)^2 + 4\tau_{xy}{}^2\right\}^{1/2} - \left\{\left(\sigma_x + \sigma_y\right)\sin\phi + 2c\cos\phi\right\} = 0 \quad (1)$$

$$\text{Coulomb}: \quad F_C = |\tau| - c - \sigma_n \tan\phi = 0 \quad (2)$$

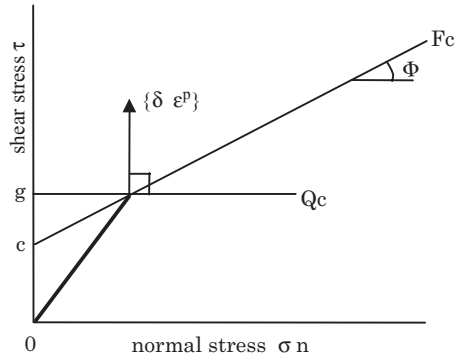

Figure 4. Yield surface and flow rule.

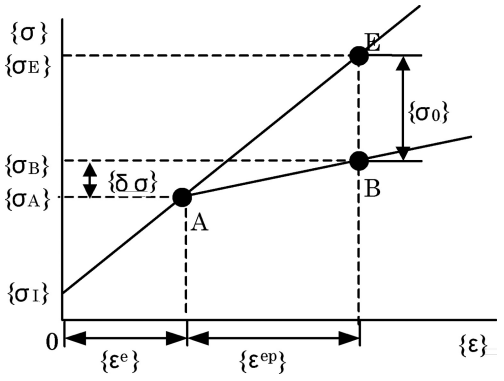

Figure 5. Initial stress method.

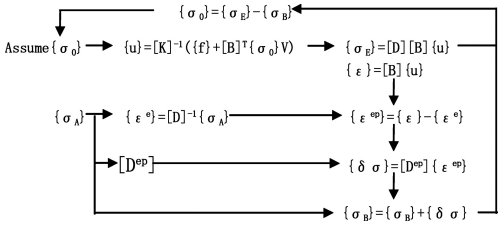

Figure 6. Flow of initial stress method.

where, $\sigma_x, \sigma_y, \tau_{xy}$: stress components in the global coordinates and σ_n, τ: normal and shear stresses in interface element.

When confining pressure σ_3 or σ_n continues increasing by the load of banking, the stress state is assumed to move on the yield surface after yielding. As shown in Figure 4, the increment of plastic strain $\{\delta\varepsilon^p\}$, when the curve moves on the yield line, was assumed to follow the non-associate flow rule with a dilatancy angle of 0. In Figure 4, Q_C is plastic potential for Coulomb interface.

Mohr-Coulomb :

$$Q_M = \left\{\left(\sigma_x - \sigma_y\right)^2 + 4\tau_{xy}{}^2\right\}^{1/2} - 2g = 0 \tag{3}$$

$$\text{Coulomb}: \quad Q_C = |\tau| - g = 0 \tag{4}$$

where, g: unnecessary parameter since plastic potential is used in a differential form. As shown in Figure 5, the entire load is applied at a single loading stage. In Figure 5, Point A shows the yield point, and Point B is the final equilibrium point. Up to Point A, the material is regarded as a linear elastic body and where, $\{\varepsilon^e\}$: elastic strain and $\{\varepsilon^{ep}\}$: elastic-plastic strain. $\{\sigma_I\}$ is the actual initial stress, $\{\sigma_A\}$, $\{\sigma_B\}$ and $\{\sigma_E\}$ are the stresses at each point, and $\{\sigma_0\}$ is the initial stress in the initial stress method, which is determined by an iteration loop. The flow of calculating $\{\sigma_0\}$ is shown in Figure 6 and where, $\{u\}$: nodal displacement vector, $[K]$: stiffness matrix, $\{f\}$: total load vector, $[B]$: matrix for calculating strain from $\{u\}$, $[D]$: stress-strain matrix, $[D^{ep}]$: elastic-plastic stress-strain matrix and V: volume of element (Arai., K. 1993). Since this numerical procedure treats only the final equilibrium state after the completion of construction, the procedure does not simulate at the construction on steps of the wall.

4 LONG-TERM STABILITY OF REINFORCED EARTH SLOPE

4.1 *Numerical analysis and field observation*

The soil parameters of the banking materials and the foundation ground used in the numerical analysis and those of the geogrid are shown in Table 4. In the table, E: elastic modulus, μ: Poisson's ratio, A: sectional area of geogrid, and T: tensile strength of the geogrid. The soil parameters of the banking materials were determined by laboratory tests. Geogrid is expressed as truss materials that bear no compressive stress. To find the final stress state of TOGA wall, the self-weight of embankment is loaded at one loading step in the numerical analysis. The calculated and monitored vertical and horizontal displacements of the ground surface and the tensile forces generated on the geogrid are compared. A comparison of the horizontal displacement of the slope surface is shown in Figure 7. Vertical displacements are compared in Figure 8. The monitored horizontal displacement at the time of completing banking is about 0.38 m the maximum at a height of about 15 m, showing that the slope bulged forward. The calculated vertical displacement values are similar to the monitored values. Since the compressive prestress was applied after banking, the calculated displacement does not agree with measured

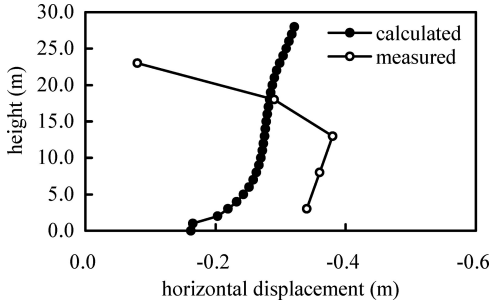

Figure 7. Horizontal displacement.

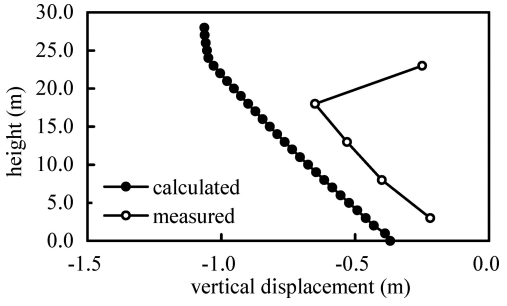

Figure 8. Vertical displacement.

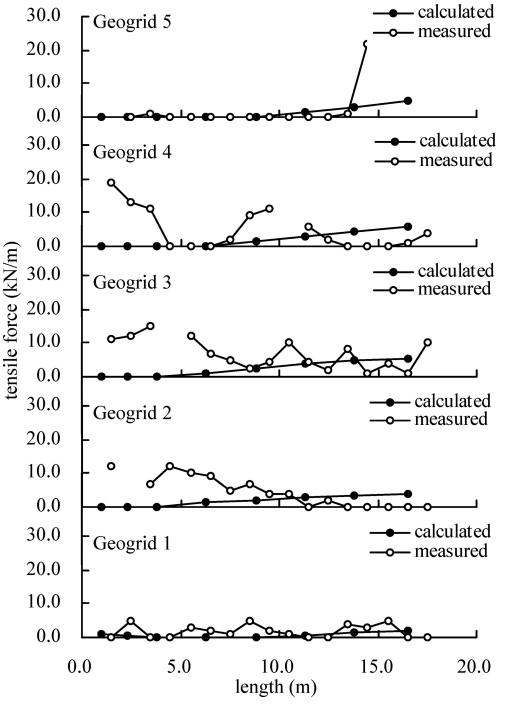

Figure 9. Tensile force of geogrid.

Table 4. Parameters using in numerical analysis.

	E(kN/m^2)	μ	c (kN/m^2)	ϕ (degree)
New embankment	1.0×10^4	0.3	30	30.0
Old embankment	1.0×10^4	0.3	0	38.0
Weathered residual rock	3.0×104	0.3	50	23.3
Highly weathered layer	3.0×10^4	0.3	60	23.3
Mid weathered layer	3.0×10^4	0.3	70	23.3
Rock (elastic body)	3.0×10^4	0.3	–	–
	E(kN/m^2)		A(m^2)	T(kN/m)
geogrid	2.6×106		5.2×10^{-4}	28.0

displacement completely. The monitored and calculated tensile forces on the geogrid are compared in Figure 9. The calculated forces are slightly different from the monitored values. Possible causes include incorrect assessment of the modulus of deformation during banking and the difficulty of monitoring the tensile forces on geogrids.

Although the results of the numerical analysis are slightly different from the monitored values in slope surface displacement and tensile force on the geogrid, the values are sufficiently close with each other in relation to a large bank height of 28 m and shows similar trends. Thus, the numerical analysis is judged to have correctly predicted the behavior of the embankment.

4.2 *Long-term stability*

To verify of long-term stability of TOGA wall, we have carried out the field observation for displacement of slope face and tensile force of geogrid after construction of TOGA wall. When the natural disasters occur such as earthquake and heavy rainfall, we are checking the settlement of road surface. We conform that the settlement of road surface and the tensile force of geogrid converge, so that we can evaluate that TOGA wall is stable state.

The stability against the failure of TOGA wall (safety factor) is predicted by using the numerical analysis. The safety factor of the earth slope is defined as follows. Generally, to represent a phenomenon of failure in which the deformation of the earth slope becomes infinitively at a certain loading step is difficult. In this paper, the failure state of the earth slope is defined that the yield finite elements connect in the earth slope like a slip surface as shown in Figure 10.

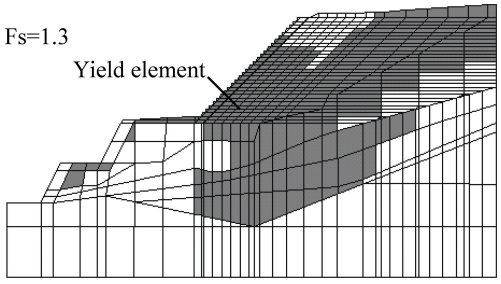

Figure 10. Distribution of yeild element.

Table 5. Effect of design parameters.

Case	Limit equilibrium method	Numerical analysis
$\gamma = 19.0\ \mathrm{KN/m^3}$ $c = 30\ \mathrm{KN/m^2}$ $\varphi = 30°$	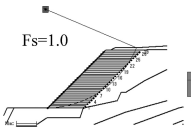	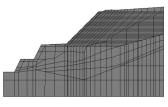
Case 2 $\gamma = 19.0\ \mathrm{KN/m^3}$ $c = 30\ \mathrm{KN/m^2}$ $\varphi = 30°$	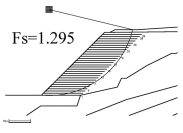	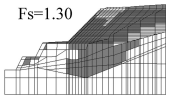

To find the failure state, hypothetical strength parameters $\underline{c}$ and are mobilized using the actual strength parameters c and ϕ and safety factor F_S as:

$$\underline{c} = c/F_S\ ,\quad \tan\underline{\phi} = \tan\phi/F_S \tag{5}$$

The safety factor of TOGA wall is $F_S = 1.3$ as shown in Figure 10, so that TOGA wall has high safety factor. We can verify that TOGA wall is stable state sufficiently based on field observation and numerical analysis over long term.

5 DETERMINATION OF SOIL PARAMETERS FOR STABILITY ANALYSIS

5.1 *Numerical analysis and limit equilibrium method*

The results of stability analysis of TOGA wall calculated using the limit equilibrium method for each design parameter and the results of the numerical analysis are shown in Table 5. The conventional design method, which uses the limit equilibrium method, assesses the tensile strength of geogrids. On the other hand, the proposed numerical procedure evaluates the stiffness of the geogrid. Thus, the values of safety factor of the two methods cannot be directly compared, but the safety factors shown in Table 5 are mutually similar. Thus, the proposed procedure should be effective for assessing the stability of actual banks.

5.2 *Evaluation of soil parameters*

When cohesion c was assumed to be zero, the proposed procedure could not calculate safety factor since the iteration procedure diverged. This occurred because the displacement and stress of the bank increased too much disabling a stable final state to be found and the iteration procedure to converge. The results of a numerical analysis conducted by assuming a safety factor of $F_S = 1.0$, which involved 50 iteration procedures, are shown in Table 5. The yield region spread throughout the bank not satisfying any of the presently arranged geogrids. Since the earth slope is confirmed to be stable based on field observation and the results of numerical analysis, designing a slope by disregarding cohesion would result in a very uneconomical design.

6 CONCLUSIONS

The long-term stability of a reinforced earth slope, which was completed about seven years ago, is examined by conducting the numerical analysis, by comparing the calculated and monitored result and by performing visual inspection. Since the results of field observation can be represented by the numerical analysis, the degree of allowance to failure is examined by calculating the safety factor, which is found to be as stable as $F_S = 1.3$. The slope is confirmed to be stable over a long period of time judging from the states of slope and highway surfaces, which are visually inspected. Safety factors calculated by the proposed procedure are compared with circular slip surface method. The comparison shows that the proposed procedure can reproduce the safety factor determined by the limit equilibrium method. The study also confirmed that design parameters should be set by considering cohesion and not by just following existing standard manual.

The slope reinforcement project was executed by carefully and thoroughly draining underground water from the foundation and the bank since the project involved large-scale banking. The reinforced earth method is likely to be highly stable and earthquake resistance in principle, but thorough drainage measures should be taken while designing and constructing reinforced earth structures to deal with intense storms observed these years. The design manual used today as a standard for designing reinforced earth structures considers cohesion very little since cohesion is difficult to assess and banking materials and soil qualities may be non-uniform, and limits the cohesion of banking materials to be $c = 10\ \mathrm{kN/m^2}$ or less.

Since most civil engineering works are public works, which must ensure safety with least expenses, economical and appropriate designs will be increasingly demanded. The authors propose a method that combines the conventional design method and FE analysis described in this paper. The new method can evaluate the safety of circular slip surfaces and safety factors as in the conventional method but only using simple soil parameters (elastic constants and c, ϕ). The method is also effective in understanding the deformation and stress states inside embankments, enabling economic and highly reliable embankment to be constructed.

REFERENCES

Ohta, H., Iwata, K., Arai, K., Kawamura, K., Nishimoto, Y., Yokota, Y. & Tsuji, S. 2006. Design and performance of a new type of reinforced earth slope, *Proceedings of the 8th International Conference on Geosynthetics*, Vol. 3: 1201–1204.

Public Works Research Center. 2000. The standard manual of geogrid reinforced soil structures.

Desai, C. S., Zaman, M. M., Lightner, J. G. & Siriwardane, H.J. 1984. Thin-layer element for interfaces and joints, *Int. J. Numer. Anal. Methods Geomech.*, Vol. 8: 19–43.

Zienkiewicz., O. C., Valliappan., S. & King., I. P. : 1969. Elastoplastic solutions of engineering problems 'initial stress', finite element approach, *Int. J. Numer. Methods Eng.*, Vol. 1: 75–100.

Zienkiewicz., O. C., Valliappan., S. & King., I. P.: 1968. Stress analysis of rock as a 'no tension' material, *Geotechnique*, Vol. 18: 56–66.

Arai., K. 1993. Active earth pressure founded on displacement field, *Soils and Foundations*, Vol. 33, No. 3: 54–67.

Yokota., Y, Arai., K., Haguro., T. & Tsuji., S. 2006. Stability analysis of reinforced soil slope considering deformation and stiffness, *Journal of Applied Mechanics JSCE* Vol. 9: 445–454.

Kubo., T. & Yokota., Y. 1999. About steel wall materials in a geogrid reinforcement soil wall construction, *Geosynthetics Engineering Journal*, Vol. 14: 72–81.

Kubo., T., Yokota., Y., Ohta., H. & Yamagami., N. 1999. Confirmation of an effect of a compression power prestress in face of slope of embankment reinforcement construction, *Geosynthetics Engineering Journal*, Vol. 14: 82–91.

Hirata., M., Iizuka., A., Ohta., H., Yamagami., N., Yokota., Y. & Omori., K. 1999 : Finite element analysis of geosynthesitics reinforcement embankment, considering dilatancy, *Proc. of Japan Society of Civil Engineering*, No.631/III-48: 179–192.

Ito., M., Yokota., Y., Kubo., T. & Arai., K. 2000. In-situ loading experiment to the protective embankment retaining wall reinforced by geosynthetics, *Geosynthetics Engineering Journal*, Vol. 15: 340–349.